BL35XU
Inelastic and Nuclear Resonant Scattering

1. Introduction

Inelastic X-ray scattering (IXS) has been the main technique at BL35XU [1]. However, the main nuclear resonant scattering (NRS) user program was moved from BL09XU to BL35XU after the end of FY2020 in accordance with the reorganization of public beamlines at SPring-8. The commissioning of modified beamline optics and NRS setups was conducted successfully in 2021A with the help of RIKEN, the optics group, and visiting researchers of JASRI, while IXS user activity was reduced in terms of beamtime. The beamline was then opened for public NRS users from 2021B, in addition to IXS users.

2. Non-resonant high-energy-resolution inelastic X-ray scattering

The IXS station of BL35XU investigates dynamics in materials using non-resonant high-resolution inelastic X-ray scattering. A Si backscattering monochromator is utilized with a high-order reflection. IXS energy resolutions are typically 1.5 meV ($h\nu$ = 21.747 keV, using the Si(11 11 11) reflection) and 3 meV ($h\nu$ = 17.794 keV, using the Si(9 9 9) reflection).

A cylindrical mirror provides a beam size of less than 100 μm (FWHM) and a beam divergence of about 0.3 mrad (H) × 0.1 mrad (V). By installing an additional focusing system using KB mirrors, a smaller beam size of less than 20 μm (FWHM) is obtained, although the divergence is increased. This small beam allows measurements on small samples. This is possible even if the samples are surrounded by other materials, such as samples under high-pressure conditions, which are surrounded by diamonds and pressure-transmitting media.

The targeted scientific fields for IXS are wide, since this method directly observes the atomic dynamics and phonons in materials, including atomic dynamics in liquids and glasses, electron–phonon correlation in correlated materials, elastic constants as functions of temperature and/or pressure, and phonon lifetimes of thermoelectric materials. Versatile measurements are conducted for both crystalline and disordered materials even under extreme conditions such as high temperature with high pressure (in a diamond anvil cell).

After the relocation of the high-heat-load monochromator (HHLM) in FY2020, an X-ray beam was introduced to the sample position on the IXS spectrometer. The beam quality was confirmed to be comparable to that before the relocation.

The performance stability for the HHLM was improved after a large amount of work by the optics group. We then investigated the effect of X-ray irradiation on the first crystal of the HHLM. We measured the rocking curve width of the silicon (3 3 3) reflection of the first crystal at 40 m downstream from the HHLM while changing the front-end slit size. The ID gap was 9.625 mm, where the energy of the fundamental harmonic is 21.7 keV. A tantalum foil of 0.15 mm thickness was placed on the detector to cut the X-ray by the Si (1 1 1) reflection. Figure 1 shows the obtained results. With a constant vertical (horizontal) gap size, the rocking-curve width increases with the horizontal (vertical) gap size. The rocking-curve width is correlated with the area of the front-end slit opening, which is an indicator of the heat load on the crystal. However, a large vertical slit gap gives a small rocking-curve width at the same area of the front-end slit opening. We can hypothesize that it comes from the fact that the distortion along the beam is more sensitive than that perpendicular to the beam. Therefore, it is concluded that the vertical slit gap should be as large as possible in the operation at a gap of 9.625 mm. According to a previous study, the rocking-curve width becomes larger, shows a maximum, becomes smaller, and then increases beyond the maximum with increasing irradiation on the crystal [2]. In contrast, the present results show neither maximum nor minimum. It could be expected that the rocking-curve width would be smaller if we made the vertical front-end slit larger than the authorized limit (0.55 mm). It might be worthwhile to perform this test with a larger power load on the first crystal of the HHLM, that is, with a larger opening area of the frontend slit or a larger ring current.

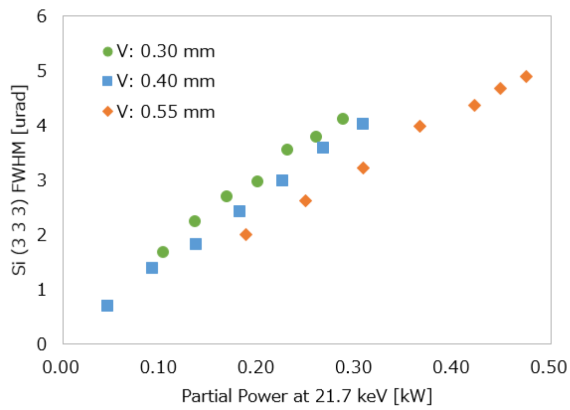

Fig. 1. Width of Si (3 3 3) rocking curve at 65 keV as a function of calculated power load on the HHLM. The power is proportional to the opening area of the front-end slit.

3. Nuclear resonant scattering

NRS provides a variety of methods to investigate atomic and electronic structures with high energy resolution, which is in the μeV-neV range. BL35XU has an advantage for NRS that high flux density is available at the excitation energy of many nuclei (see Fig. 3 in Ref. [3]), owing to the specialized insertion device. In addition, during the relocation of the instrumentations and commissioning, some instrumentations have been installed and updated [4]. The updates will accelerate the progress of the research using the NRS method.

BL35XU was highly optimized for IXS work, and this has also been beneficial for the NRS program. In particular, the short, 20 mm period ID at BL35 provides 2 to 3 times more flux than a conventional ID, except for a dead region between 29 and 43 keV. This provides a higher flux density to the sample at the energies of many Mössbauer nuclei. For user experiments using the inaccessible ranges of the BL35 ID, JASRI continues experimental support at BL19LXU.

Figure 2 shows the new layout of BL35XU. In the optics hutch, the HHLM was moved 3.3 m upstream to place an optical table for high-resolution monochromators (HRMs). The cooling power and the stability of the HHLM were improved by the optics group to improve performance under high power, such as at 14.4 keV, which is the excitation energy of ^{57}Fe. There are six HRMs with X-stages, which make each HRM inserting/removing in the beam path easy. A Pt-coated bent cylindrical mirror (14 mm sagittal radius) is installed downstream of the HRMs, a setup similar to that used at BL43LXU. The focal length can be changed by controlling the incident angle and the bending depending on the energy. The focused beam can be obtained in the NRS1 hutch for up to ~30 keV with the focal length of 3 m and

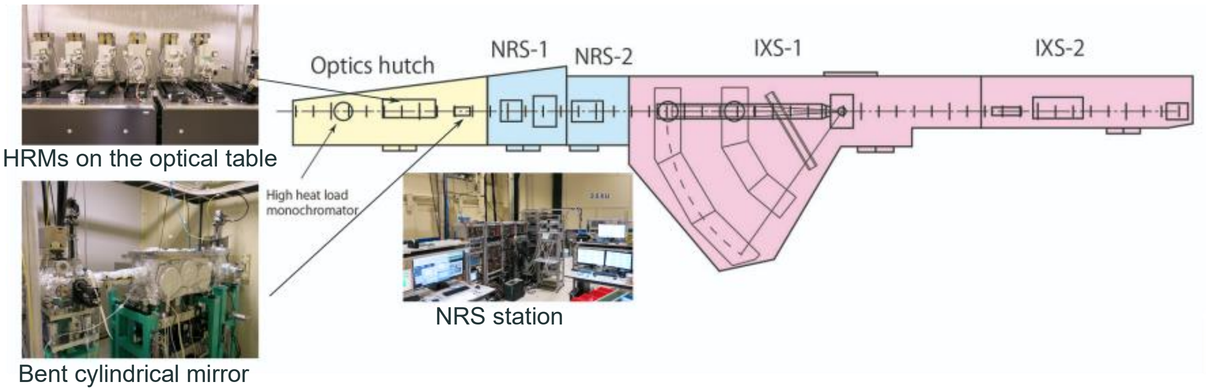

Fig. 2. New layout of BL35XU.

in the NRS2 hutch for up to ~80 keV with the focal length of 8 m. The beam size at the focal point in the NRS1 hutch becomes ~20 µm (vertical) and ~50 µm (horizontal) for 14.4 keV.

The spectrometers are installed in the experimental hutches, namely, the NRS1 and NRS2 hutches, as shown in Fig. 2. There are two optical tables in the NRS1 hutch. A velocity transducer with a low-vibration-type pulse-tube cryostat for energy domain Mössbauer spectroscopy (EDMS) is on the table downstream of the NRS1 hutch. For nuclear forward scattering (NFS) and EDMS measurements, samples are placed on the table upstream of the NRS1 hutch. A ^{57}Fe HRM with a resolution of 0.8 meV is also on the downstream table in the NRS1 hutch and delivers the monochromatized X-ray to the NRS2 hutch.

The quasi-elastic scattering (QES) spectrometer and a pulse-tube-type cryostat for nuclear inelastic spectroscopy (NIS, also sometimes called nuclear resonance vibrational spectroscopy, NRVS) are placed on an optical table in the NRS2 hutch. These instrumentations except for the upstream table in the NRS1 hutch are placed permanently. This makes the switching of the equipment easy and quick. When users bring a new instrument, they can install it upstream of the NRS1 hutch.

Table 1 shows the flux measured at BL35XU and the factors of that at BL09XU. As shown in Table 1, flux with a factor of 2 or more were obtained for almost situations. Since the HRMs are sensitive to temperature, a high-precision air conditioner is installed for the optics and NRS1 hutches. This makes good energy stability of the monochromatized X-ray; for example, the stability that is within ±0.1 meV during a half day with the 0.8 meV ^{57}Fe HRM is realized.

Table 1. Evaluated flux from PIN current values measured at BL35XU and the factors compared with those of BL09XU (same table as in Ref. [4])

Nuclei	Energy [keV] (Resolution)	Flux [× 10^{10}ph/s]	Factor [BL35/BL09]
^{57}Fe	14.4 (6 meV)	16	2.1
	14.4 (3.5 meV)	5.3	1.9
	14.4 (2.5 meV)	3.3	2.4
	14.4 (0.8 meV)	0.56	2.1
^{151}Eu	21.5 (1.2 meV)	1.5	3.2
^{119}Sn	23.9 (1.5 meV)	0.38	3.4
^{61}Ni	67.4 (~0.35 eV)	7.4	2.3

Fukui Hiroshi, Nagasawa Nobumoto, Uchiyama Hiroshi, and Yoda Yoshitaka
Precision Spectroscopy Division, JASRI

References:

[1] Baron, A. et al. (2000). *J. Phys. Chem. Solids.* **61**, 461.
[2] Chumakov, A.I. et al. (2014). *J. Synchrotron Radiat.* **21**, 315–324.
[3] Yoda Y. et al. (2021). *SPring-8/SACLA Communications.* **26**, 329–334.
[4] Yoda Y. et al. (2021). *SPring-8/SACLA Communications.* **26**, 450–451.